



Detection and Analysis of Critical Interactions in Illegal U-Turns at an Urban Signalized Intersection

Clemens Schick Tanz¹ · Kay Gimm²

Received: 15 October 2024 / Revised: 19 December 2024 / Accepted: 9 January 2025
© The Author(s) 2025

Abstract

Before automated vehicles can safely operate in real-world traffic, it is crucial to ensure their reliability not only in normal conditions but also in rare and critical situations, such as traffic conflicts. Understanding these critical situations is essential for generating test cases that ensure robust system performance. However, current models of real-world traffic behavior in such situations are limited. This study addresses this gap by detecting rare critical situations at an urban signalized intersection, analyzing road user behavior, and deriving relevant parameter distributions through a long-term analysis of naturalistic trajectory data. Specifically, we focus on interactions between motorized road users (MRU) and crossing vulnerable road users (VRU) in illegal U-turn scenarios. Using over 180 days of video recordings, we extracted 9 million trajectories and identified four critical MRU–VRU interactions utilizing Surrogate Safety Measures and deceleration metrics. The analysis reveals that these interactions occur when the VRU traffic light switches from red to green. In addition, we descriptively model the driving behavior to generate parameter distributions for U-turn scenarios. Unlike previous studies, we differentiate between object classes, allowing us to effectively illustrate variations in curve radius—such as median values of 8.1 m for cars, 9.7 m for vans, and 14.3 m for trucks. Our results demonstrate an approach for modeling traffic participant behavior using large-scale trajectory data, showcasing a use case of data science in transportation and contributing valuable insights for simulation-based testing and scenario generation in automated vehicle development.

Keywords Long-term data analysis · Naturalistic trajectory data · Descriptive behavior modelling · U-turn

Introduction

Automated vehicles (AVs) are expected to change the transportation system dramatically and reduce the number of crashes (Fagnant and Kockelman 2015). However, AVs cannot be expected to be reliable and safe in every situation (Dixit et al. 2016; Martens and van den Beukel 2013). Although it was found that collisions with pedestrians are less common for AVs than for conventional vehicles (Petrović et al. 2020), the development of AVs is not yet advanced enough to reach an acceptable level of trust in the

broad society. Therefore, the validation of autonomous vehicles is essential to ensure that the AVs behave as expected in rare critical situations and increase trustfulness.

The testing of AVs is conducted worldwide, with significant efforts aimed at bringing AVs closer to market release. According to Riedmaier et al. (2020), the scenario-based approach is a promising method for safety assessment in simulation. As the name suggests, this approach involves testing AVs in multiple scenarios by varying the parameters of each scenario, all within virtual simulations. Accurate parameterization of these scenarios is crucial for realistically simulating both, the vehicle under test and the surrounding traffic participants. Naturalistic trajectory data offers great potential for deriving realistic parameter distributions, as it captures real-world traffic conditions with a high level of detail. However, since AVs currently represent only a small fraction of vehicles in everyday traffic, naturalistic trajectory data and scenarios recorded by AVs themselves are scarce. This lack of data makes it challenging to compare

✉ Clemens Schick Tanz
clemens.schickanz@dlr.de

Kay Gimm
kay.gimm@dlr.de

¹ German Aerospace Center (DLR), Institute of Transportation Systems, Berlin, Germany

² German Aerospace Center (DLR), Institute of Transportation Systems, Brunswick, Germany

rare critical situations and to identify the situational factors that contribute to their occurrence.

Infrastructurally recorded trajectory data provides an advantage in this context, as it captures similar scenarios multiple times at the same location, making it easier to derive different variations of a scenario. However, to the best of the authors' knowledge, large data sets from specific locations have not yet been utilized to prepare truly rare events for scenario-based testing.

Our contribution addresses this research gap and is divided into two parts. First, we provide a methodology to detect illegal U-turn scenarios in real-world trajectory data. This methodology enables the extraction of comprehensive parameter distributions, which can be subsequently employed to model logical scenarios involving illegal U-turns. Second, we show, that for rare critical scenarios, called corner cases (CC), a vast amount of naturalistic trajectory data is required to ensure their inclusion in the data set. For this, we detect the CCs in a data set from the Application Platform for Intelligent Mobility (AIM) Research Intersection (Knake-Langhorst and Gimm 2016) and analyze the CCs to identify factors that promoted criticality.

All in all, this paper demonstrates how infrastructurally recorded data can be leveraged, using the example of an illegal U-turn, to address the research gap. It is emphasized that this represents just one illustrative scenario and forms only a part of a broader scenario database of rare events. Such a database is essential for validating and securing automated driving functions, particularly against illegal behavior in urban environments. By integrating this approach, we aim to contribute to the systematic preparation of rare but critical scenarios for scenario-based testing.

The remaining paper is structured as follows. “[Literature Review](#)” section summarizes related work in the relevant fields of research. In “[Methodology](#)” section, the proposed methodology for U-turn scenario identification and analysis is introduced. “[Results and Discussion](#)” section presents and discusses the results of applying our method to a data set. Finally, the work concludes with a summary, including an outlook on future work in “[Conclusion](#)” section.

Literature Review

The research fields of scenario-based testing, trajectory analysis, and modelling of traffic behavior have been studied for many years. Therefore, the relevant literature is presented in the following subsections.

Scenario-Based Testing

This work aims to provide parameter distributions for a *logical scenario*. To ensure a common understanding of the term

logical scenario, we take over the following definition of a *scenario*. “A scenario describes the temporal development between several scenes in a sequence of scenes. Every scenario starts with an initial scene. Actions & events as well as goals & values may be specified to characterize this temporal development in a scenario. Other than a scene, a scenario spans a certain amount of time” (Ulbrich et al. 2015).

Three years after defining the term *scenario*, Menzel et al. (2018) differentiated the following three different scenario levels of abstraction. The most abstract is the *functional scenario*, which describes all entities and their relationships using a linguistic scenario notation. Somewhat less abstract are the *logical scenarios*, which are scenarios composed of parameter ranges or probability distributions of parameters and even parameter correlations. The less abstract one is the *concrete scenario* that can be derived by choosing a concrete expression for each parameter of a logical scenario.

In the following paragraph, we explain the connection between our contribution and scenario-based testing. The primary contribution of this study lies in the identification of various concrete scenarios in the large trajectory data set and their aggregation into a logical scenario, which serves as input for a scenario database. These scenarios can subsequently be employed by other researchers to evaluate the performance of automated driving functions, particularly those designed to handle non-compliant behaviors of other road users in urban settings. The calibration of automated driving functions can be facilitated using the methodology described in Fraikin et al. (2020). For further insights into scenario-based testing, please refer to (Cai et al. 2022; Zhong et al. 2021; Riedmaier et al. 2020; Nalic et al. 2021).

Corner Cases in the Context of Automated Driving

The development of automated driving functions continues to advance. Now that AVs can maneuver through simple situations with increasing reliability, the focus of the research is shifting to the reliability of the functions in complex, critical, and rare situations, as driving functions must perform as expected in these situations, commonly referred to as *corner cases* (CCs). According to Bogdoll et al. (2021), in the context of automated driving, a CC represents data that occurs irregularly, describes a potentially critical situation, and rarely, if ever, occurs in data sets. As AVs become more widespread, the likelihood of vehicles encountering such unexpected situations increases. Therefore, it is crucial to consider CCs in the development of AVs.

To handle the various occurrences of CCs in a structured manner, efforts are being made to systematize them. For example, Breitenstein et al. (2020) propose a grouping for image recognition according to the level of complexity in detecting CCs. These levels are ordered by ascending complexity, the pixel-, domain-, object-, scene-, and

scenario-level. In addition, there is a guideline for detecting CCs at different levels (Breitenstein et al. 2021). Heidecker et al. (2021) take up the results of the previously mentioned work and extend it by distinguishing the CCs concerning the sensor modality (camera, lidar, and radar) to provide an application-oriented conceptualization.

To the best of our knowledge, none of the existing studies incorporate CCs in the analysis of trajectory data. Only two studies explicitly address this topic (Rösch et al. 2022; Schicktanz and Gimm 2025). In Rösch et al. (2022), CCs in trajectory data are categorized according to their source of failure and data that is needed to detect the CC. The authors combine this information to propose a taxonomy of CCs in trajectory data for autonomous driving and show examples. Schicktanz and Gimm (2025) analyze scenarios involving hard braking maneuver, red-light violations, and near misses under adverse conditions. In comparison, this study does not address the extraction of parameter distributions for logical analyses. The overviews of Meng et al. (2019) and Saul et al. (2014) show that there are different approaches for detecting rare situations such as trajectory outliers or atypical trajectories. However, as CCs in trajectory data require a rare and critical traffic situation, detecting only rare situations is not enough. The same holds for the identification of only critical scenarios that can be detected using Surrogate Safety Measures (SSM), because they do not need to be rare (Wang et al. 2021). In addition, even the identification of safety-relevant scenarios (Weber et al. 2019), does not take into account that the scenarios need to occur irregularly to be a CC. Finally, the use of a large data set, such as the one utilized in this study is essential for identifying rare and critical real-world situations.

Data Sets

To show that our data set is comparable large, we compare it with other publicly available ones in the following. Public data sets can be divided by the type of recording into three classes. Either car, infrastructural mounted cameras, or drones recorded them. Another class of data sets is scenario data sets which contain the extracted scenarios.

Dozens of open data sets collected by cars on public roads are reviewed (Guo et al. 2020; Kang et al. 2019; Yin and Berger 2017). According to Guo et al. (2020), the largest publicly available data set that was recorded by a car and collected data over a long period is the Oxford RobotCar data set. It was recorded to capture the same spots in varying contexts (e.g., weather, time of day, traffic volume) and contains over 100 sequences of a consistent route that were recorded twice a week for 1 year (Maddern et al. 2017).

The most widely used publicly available infrastructurally collected trajectory data set is the “Next generation simulation (NGSIM)” trajectory data set (Kovvali et al. 2007).

The data set has been widely used for empirical traffic flow analysis and was collected in 2006 with a size of several thousand trajectories with a length of 600 m and a temporal extent of 15 min (Seo et al. 2020). According to Seo et al. (2020), the largest publicly available infrastructurally recorded data set to the date of publication is the Zen Traffic Data data set, with a scope of 18,000 trajectories, each of them two kilometers in length, from records of 5 h. Smaller trajectory data sets recorded from stationary cameras have also been made publicly available recently (Cres et al. 2022; Zernetsch et al. 2022).

The first publicly available trajectory data set recorded by a drone was the Stanford drone data set (Robicquet et al. 2016), with 10,240 trajectories from 9 h of recording. Later, the highD data set was recorded by drones flying 16.5 h over highways and extracting 110,000 vehicle trajectories at six different locations (Krajewski et al. 2018). And finally, the openDD data set was published as the largest drone data set to date of publication in 2020, containing 84,774 trajectories from 62.7 h of recording (Breuer et al. 2020).

The aforementioned data sets contain trajectories. Efforts have already been made to extract scenarios from data sets and build up databases of scenarios instead. There is a so-called StreetWise database that contains real-world traffic scenarios from multiple continents (Elrofai et al. 2018). According to StreetWise, the process of extracting scenarios from data sets is also referred to as scenario mining. In addition, other scenario databases have been mined by others (Klitzke et al. 2022; Zhu et al. 2018).

Finally, we found that all these publicly available data sets and databases have a lower amount of data from a specific place than the data set examined in this work consisting of over 4000 h of recordings and over 9 million trajectories from a single intersection.

Critical Interactions in Road Traffic

This work aims to contribute to the understanding and mitigation of critical interactions in the context of road traffic safety. As a basis for critical interactions, the term *interactions* need to be understood first. Therefore, we take over the following definition. “A situation where the behaviour of at least two road users can be interpreted as being influenced by the possibility that they are both intending to occupy the same region of space at the same time in the near future”(Markkula et al. 2020).

The identification of critical interactions provides valuable insights that can contribute to preventing similar interactions in the future. This approach is supported by findings from previous research, such as the study by Habibovic et al. (2013) conducted in Japan, which highlights the importance of understanding the dynamics of road user interactions. Their research showed that incidents involving cars and

pedestrians result from drivers failing to recognize pedestrians or unexpected pedestrian behavior. By focusing on critical interactions, we build on this foundation, aiming to identify patterns and contributing factors that can inform targeted safety measures and reduce the likelihood of such incidents.

Other studies delve into the modelling and evaluation of behavior within safety-critical interactions. For instance, Abdelhalim and Abbas (2022) employs an optimal velocity model to capture safety-critical driver behavior at signalized intersections. The evaluation of driving behavior's safety aspects is addressed theoretically, while behavior is systematically classified through simulation in Yang et al. (2022).

U-Turn Modelling

The modelling and simulation of U-turns received particular attention in research when median U-turns were introduced to replace left turns at busy intersections and thereby increase traffic safety (Liu et al. 2012). Therefore, various studies from different countries and different types of intersections exist and are about the influence of U-turns on traffic flow and efficiency in general (Al-Masaeid 1999; Mazaheri et al. 2022; Mikhailov and Shesterov 2020; Liu et al. 2007; Leng et al. 2009; Sun et al. 2019; Peng and Yujing 2020; Shahi and Choupani 2009; Olarte et al. 2011; Che Puan et al. 2015). In addition, the detection of illegal U-turns has been investigated already (Song and Lee 2014; Wang et al. 2018; Rathore et al. 2021).

In one study safety related topics are studied, too. Olarte et al. (2011) built regression models based on traffic density and volume. They also simulated U-turns using software called VISSIM (Fellendorf 1994) to show that the number of conflicts rises when a specific traffic volume is exceeded. Other studies used the simulator VISSIM for simulating U-turns, too (Peng and Yujing 2020; Sun et al. 2019; Leng et al. 2009; Liu et al. 2012). Another microscopic traffic simulation software called SUMO “Simulation of Urban Transportation” (Krajzewicz 2010) was used to generate U-turn scenarios (Yue et al. 2020). Although the authors describe that the scenarios can be used for scenario-based testing, the resulting data is generated by simulation and does not necessarily represent real-world behavior.

In some studies, real-world data are used to analyze the interactions with the oncoming traffic. Che Puan et al. (2015) use stationary video recordings of more than 2,000 U-turning vehicles and analysis software to extract the gap acceptance of U-turning vehicles to the oncoming traffic (Che Puan et al. 2015). They found that at high traffic volumes, the U-turns often lead to a reduced traffic flow in oncoming traffic. Mohanty and Dey (2020) model the interaction with the oncoming vehicles, too. They focus on their lane change behavior as a reaction to the U-turning vehicles.

All in all, many references use traffic efficiency-related parameters such as traffic volume, flow, and density. Some of them, like gap acceptance (Che Puan et al. 2015), percentage of left turns (Leng et al. 2009) and median width (Liu et al. 2007), are used only by single references. Furthermore, there exist two studies using kinematic parameters like the turning speed of U-turns (Liu et al. 2012; Zheng et al. 2009). In summary, there is an overlap with other studies in just one parameter utilized for U-turn modelling, namely, the parameter “speed”, which was used in previous studies (Liu et al. 2012; Zheng et al. 2009). Our trajectory data offers insights into microscopic traffic, allowing us to utilize more detailed parameters, such as curve radius and vehicle heading. These parameters are not used by others.

Furthermore, our research focuses exclusively on interactions between U-turning vehicles and vulnerable road users (VRUs) at signalized intersections, a topic not explored in previous literature. Specifically, our study delves into how to model this scenario for scenario-based testing and examines the differences in U-turning behavior across different object classes, aspects that have not been investigated before.

Summary

In summary, this study distinguishes itself from previous work in two key aspects. Unlike prior studies, it utilizes a large real world data set to capture a specific rare scenario, enabling the extraction of detailed parameters. This approach allows for the use of multiple parameters, such as speed, acceleration, and heading, and facilitates comparisons across different object classes, providing a more comprehensive understanding of the scenario.

Methodology

In the following, we present the steps to descriptively model the U-turning vehicles and detect the corner cases. All steps were executed using our own Python package “Traffic Analysis and Situation Interpretation” (TASI) (Klitzke and Schicktanz 2024). Parts of the software are publicly available at github.com: <https://github.com/dlr-ts/tasi>.

In the first step, relevant elements of the OpenDRIVE map (Scholz 2020) are extracted as virtual loops (VLs) to model the routes of the U-turning motorized road users (MRUs) and the crossing VRUs. The data set is then filtered by identifying which trajectories intersect with these VLs. Trajectories that intersect all relevant VLs of a route are assigned to the corresponding route. Trajectories that do not intersect all loops of a specific route are excluded from the data set. This filtering process is applied to both MRU and VRU trajectories.

To descriptively model the U-turning MRU, three different sorts of parameters are defined, and correlations between the parameters are analyzed. The first group of parameters models the general aspects of the scenario and includes the object class (car, van, truck) and the descriptive statistics (minimum, maximum, mean, median, and standard deviation) of the parameters velocity and acceleration.

The second group of parameters describes the kinematic behavior of the U-turning traffic participant during the maneuver. To achieve this, the U-turn is divided into sections using VLs which are strategically placed at key locations: at the entry point to the intersection, the entry point to the oncoming lane, the entry point to the VRU crossing, and the exit of the VRU crossing. These positions are chosen, because they mark critical conflict points, where the U-turning vehicle interacts with conflicting traffic streams. The parameters heading, speed, acceleration, and the distance to the reference line are then calculated at each intersection between a trajectory and a VL. In addition, the time required for a vehicle to pass the area between two consecutive VLs, as well as the total time between the first and last VL are calculated to describe the temporal component of the scenario. For a visualization of the VLs, see Fig. 2.

The third group of parameters contains only the post-encroachment time (PET), which is used to model the interaction and criticality between the participants of the scenario. The PET is defined as the time between the moments when two road users pass the same position (Allen et al. 1978). We chose the parameter PET, because it is widely regarded as an effective metric for assessing the severity of interactions, particularly in safety-critical scenarios. Furthermore, it facilitates a detailed analysis of temporal spacing, allowing for consistent comparisons across various traffic situations and providing valuable insights into conflict dynamics (Kassim et al. 2014). In the scenario under investigation, the PET is calculated between all U-turning and relevant VRU trajectories. A VRU trajectory is considered relevant if it coincides temporally with the MRU trajectory. In addition to temporal filtering, special filtering is also applied. Specifically, only intersections located in the area of the VRU crossings of the western exit are considered relevant to the scenario, while intersections at the entrance of the MRU to the intersection are excluded from this study.

The result of this filtering process is a compilation of PET values for pairs of road users. Based on these values, *encounters* are defined as instances, where road users pass each other with a PET between 2 and 5 s. Situations with an absolute PET value below 2 s are categorized as *interactions*. This threshold was chosen based on the assumption that road users passing a conflict point within this time window would have mutually recognized each other, thus interacting in a meaningful way. Next, we assessed whether the road users involved in these interactions decelerated with

more than 1 m/s^2 . If this condition was met, the interaction was categorized as *critical*.

The threshold of 1 m/s^2 for deceleration was determined after reviewing the situations filtered by PET. We found that all critical interactions exceeded this deceleration value. This threshold for braking acceleration depends on the speed of the vehicle, and thus had to be empirically determined for the U-turn scenario. The selected PET threshold are also based on findings from previous studies (Peesapati et al. 2013, 2018; Ansariyar 2023), ensuring alignment with established research in the field. To validate the results, the filtered videos were thoroughly reviewed, allowing for a detailed check of the observed interactions. This approach ensures that the chosen parameters are both theoretically grounded and empirically verified. This validation step, involving the review of video recordings, was also conducted to filter out inaccuracies in trajectory data and to enhance the robustness of the methodology.

In addition, the video recordings of the interactions were analyzed to identify the parameters that contributed to the interaction. These parameters are then correlated with the PET values to assess the statistical relationship between the parameters and the SSM. The correlation between two random variables, X and Y , is described by the Pearson correlation coefficient $\rho_{X,Y}$ (Pearson 1895), as defined in the following equation:

$$\rho_{X,Y} = \frac{\text{cov}(X, Y)}{\sigma_X \sigma_Y} \quad (1)$$

with $\text{cov}(X, Y)$ is the covariance of the random variables and σ_X and σ_Y are their standard deviations (Benesty et al. 2009). In the following a correlation of $0.3 \leq \rho_{X,Y} < 0.5$ is considered “weak”, $0.5 \leq \rho_{X,Y} < 0.8$ is considered “moderate” and $\rho_{X,Y} \geq 0.8$ is considered “strong”.

Results and Discussion

This section applies the described method to a data set, with the findings discussed in detail. First, the examined data set and scenario are introduced. The modeling of U-turns and the detection and analysis of critical collisions (CCs) are then presented.

Data Set

The data set used in this study was recorded at the AIM Research Intersection, which is part of the Institute of Transportation Systems at the German Aerospace Center. The intersection is an urban multi-lane intersection located on the inner-city ring road of Braunschweig, Germany. It is equipped with 14 vertical stereo-camera systems positioned

at various locations to ensure comprehensive coverage and minimize occlusions of traffic participants. The data set consists of 4553 h, or approximately 190 days, of video recordings, spanning from January 21 to September 5, 2019. During this period, 9,166,560 trajectories of traffic participants were extracted. For more information about data recording and preparation please refer to (Knake-Langhorst and Gimm 2016). The analyzed data set is significantly larger than other publicly available data sets captured by infrastructure (Cres et al. 2022; Zernetsch et al. 2022; Seo et al. 2020), with the largest data set (Seo et al. 2020) containing 18,000 trajectories from 5 h of recordings. One day of data from the AIM Research Intersection is publicly available (Schickanz et al. 2024).

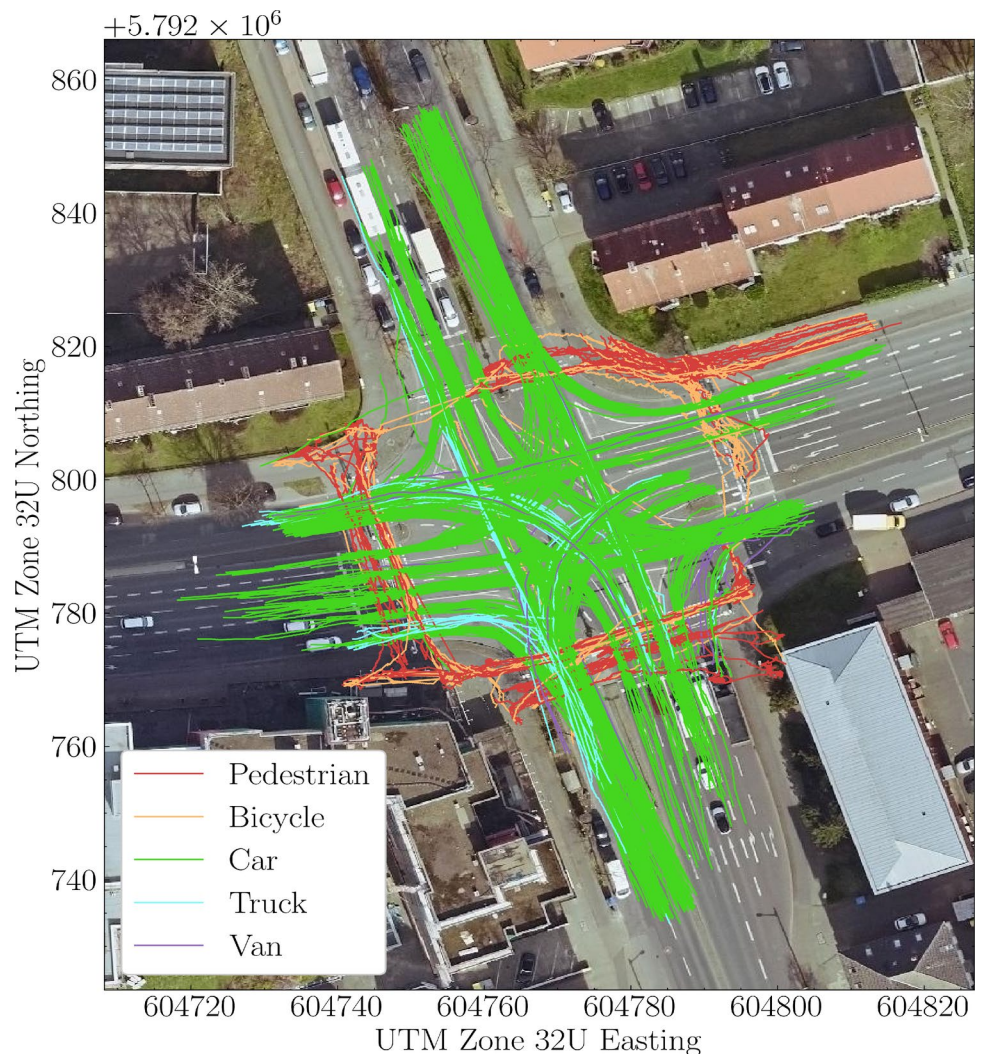
The trajectories of the data set include kinematic information, such as position, velocity, and acceleration along the x and y axes in the Universal Transverse Mercator (UTM) coordinate system, recorded at a frequency of 25 Hz. In addition, the data set encompasses estimations of the road users' dimensions (length, width, and height), which are used to

classify the objects into one of the following categories: car, van, truck, pedestrian, or bicycle. The resulting probabilities associated with each object's classification are provided for each timestamp within the trajectory data. A portion of the center position values from the trajectory data set is shown in Fig. 1. All trajectory figures are oriented northwards.

In the west of the intersection, executing a U-turn is prohibited by a traffic sign. Nevertheless, some traffic participants violate this regulation and perform U-turns from the lane designated for left-turning vehicles. As this maneuver involves an unprotected left turn, vehicles must wait for oncoming traffic from the east to pass or for a sufficiently large gap between two oncoming vehicles to execute the turning maneuver safely. Typically, after yielding to oncoming traffic, the U-turn is completed by exiting the intersection to the west.

This scenario was selected, because it represents a frequently occurring rule violation at the intersection, making it suitable for descriptive modeling and statistical correlation analysis. Since the data from the traffic lights are

Fig. 1 Trajectories from traffic participants on the AIM research intersection recorded between 9 and 11 PM on the 21st of January 2019. Background image reference: © The City of Brunswick, Department Geographic Information



not considered, the scenario shares many similarities with U-turns at unsignalized intersections. In addition, the U-turn is only prohibited at the western entrance to the intersection, meaning that data from permitted U-turns at the other entrances cannot be used in this study.

Trajectory Filtering

The trajectories of U-turning vehicles must be filtered from the data set using VLs extracted from the digital map of the intersection (Scholz 2020). Since the VLs are manually selected for this U-turn scenario, automating the extraction of the VLs could be a valuable component of further work, facilitating the application of the methodology to other data sets. The VLs and the corresponding trajectories that intersect all VLs are visualized in Fig. 2.

The 1st virtual loop (green) is placed along the inner edge of the bicycle crossing. This position was chosen, because, at this point, all U-turning MRUs are detected for the first time by the system at the latest. Specifically, the left lane border of the oncoming traffic (east to west) is the next critical marking (red). In addition, the U-turning MRUs exit the intersection by passing the VRU crossing, so the inner (orange) and outer (yellow) edges of this crossing are also considered as VLs. An area between two consecutive loops is referred to as a *section* in the following. By calculating the intersections between U-turning MRU trajectories and VLs, 4,051 trajectories (0.04% of the data set) of illegal U-turns are detected.

Using the same methodology but with different VLs, the relevant trajectories of VRUs are extracted from the data set. For this extraction, the lane borders at transitions from dropped curbs to roadways are modeled as VLs, and intersections with the trajectories are computed. Some of these extracted trajectories, which intersect both VLs, are shown in Fig. 3.

Fig. 2 All trajectories of U-turning vehicles in the west of the intersection. Background image reference: © The City of Brunswick, Department Geographic Information

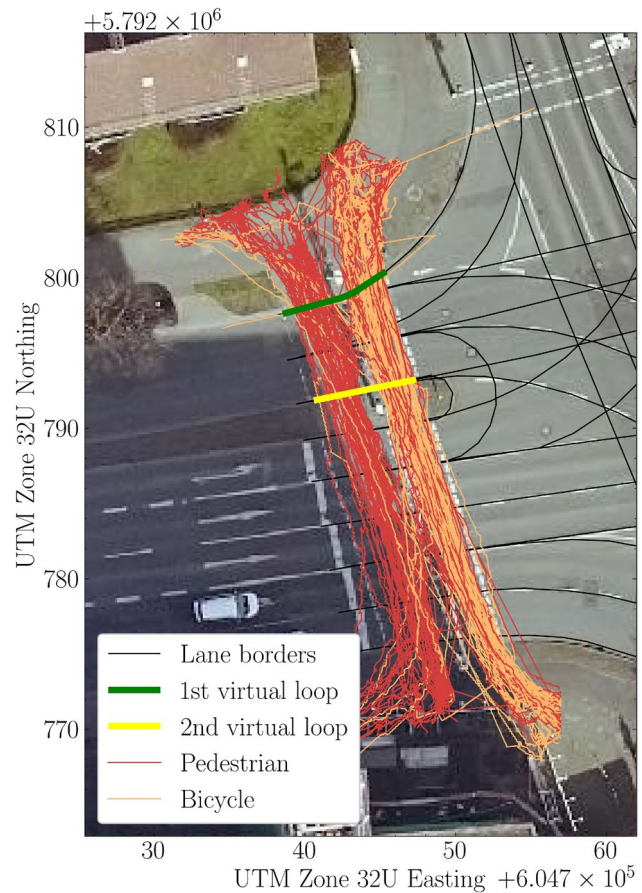
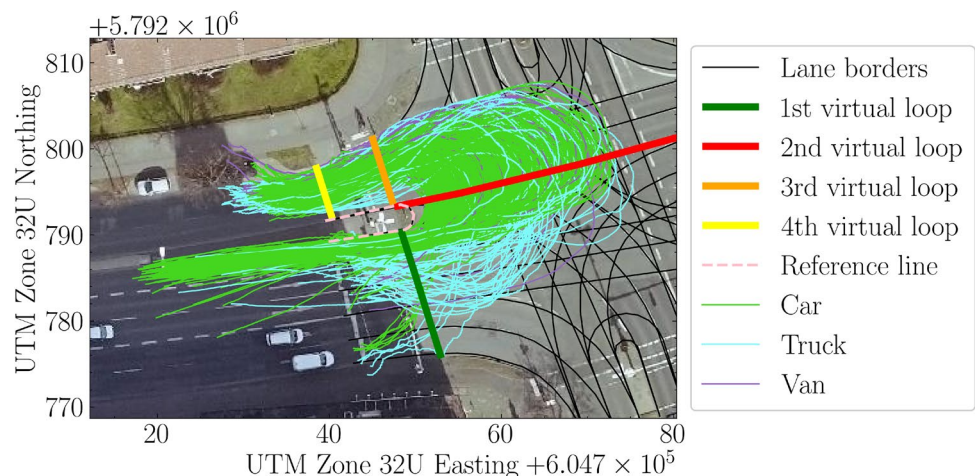


Fig. 3 VRU trajectories of the first 10 h in the west of the intersection. Background image reference: © The City of Brunswick, Department Geographic Information

Descriptive Model of a U-Turn

This section presents an overview of the general characteristics of U-turns, the kinematic parameters at the VLs, and interactions with VRUs.

General Aspects

The data set includes 3,663 U-turn trajectories of cars, 244 U-turn trajectories of vans, and 144 U-turn trajectories of trucks. Analysis of the time of day when these U-turns occur (see Fig. 4) reveals that, on average, vans (10:35 AM) and trucks (9:20 AM) perform U-turns earlier in the day than cars (01:00 PM). This pattern may be attributed to the fact that vans and trucks are more commonly used as work vehicles during the day, whereas private cars are predominantly used in the evening when fewer work-related trips occur.

In Table 1, we present the mean values of the descriptive statistics of the velocities for each trajectory. Specifically, v_{min} represents the mean of all minimum velocity values across the trajectories. Based on this analysis, one might expect smaller MRUs, such as cars, to exhibit higher velocities than bigger MRUs, such as trucks. However, this expectation is not supported by the data. As shown in Table 1, the minimum, mean, and median velocities of trucks are higher than the corresponding values for cars. A potential explanation for this observation could be the later detection of trucks, resulting in shorter waiting times before crossing the 2nd VL. Reduced waiting time decreases the number of low-velocity values, thereby elevating the mean and median velocities. However, this reasoning does not apply to vans, which consistently show lower velocities than cars, as initially anticipated. This observation raises the possibility of increased data error, as trucks, being large road users, present significant challenges for accurate detection. Extensive data preprocessing could improve data quality, leading to more realistic outcomes and enhancing the contribution of this study. Although trucks take approximately twice as long as cars to traverse the second (7.0 s vs. 3.2 s) and third section (1.9 s vs. 1.2 s), their time for the first section (11.3 s vs. 11.0 s) is not significantly longer. This is because the

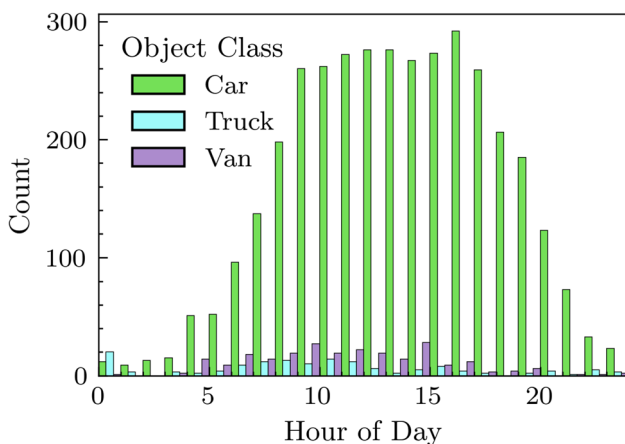


Fig. 4 Number of U-turns per hour of the day

Table 1 Descriptive statistics of velocity for different object classes in m/s

Object class	v_{min}	v_{mean}	v_{med}	v_{max}	v_{std}
Car	0.44	2.66	2.12	8.15	2.03
Van	0.34	2.44	2.05	7.61	1.81
Truck	0.71	2.69	2.44	6.87	1.45

Bold value represent the maximum values in each respective column

duration required for the first section is primarily influenced by waiting time.

The descriptive statistics analysis of the measured acceleration values per trajectory supports the assumption that, on average, cars exhibit higher acceleration than larger MRUs (see Table 2). This pattern holds for all descriptive statistics except for the minimum acceleration. Since many trajectories include data from scenes, where the MRUs are stationary, the minimum acceleration for numerous trajectories is 0. As a result, the mean minimum acceleration across all object classes is 0.

Kinematic Parameters at Virtual Loops

The VLs shown in Fig. 2 are used not only for filtering the trajectories but also for extracting the heading (0° to the east, increasing counterclockwise), the time and kinematic parameter (position, velocity, and acceleration) at the intersection of the trajectories with the VLs. Four of the five variables are determined at each of the four loops, while the "duration until the next loop" is calculated only for the first three loops, as it cannot be computed for the last one. This results in a total of 19 parameters. Based on this data, the kinematic behavior of the U-turning vehicles is descriptively modeled. In Table 3, the mean parameter values of cars are presented.

In addition to the 19 parameters from Table 3, the overall duration of the U-turn is analyzed as the 20th parameter. The results show that larger MRUs take longer to complete a U-turn (cars 15.41 s, vans 18.58 s, trucks 20.21 s). This difference mainly comes from the duration of the second section (cars 3.26 s, vans 4.86 s, trucks 7.02 s). In contrast, the first section shows smaller differences (cars 10.98 s, vans 12.28 s, trucks 11.31 s). This indicates that, regardless of object class, the average waiting time for oncoming traffic

Table 2 Descriptive statistics of acceleration for different object classes in m/s

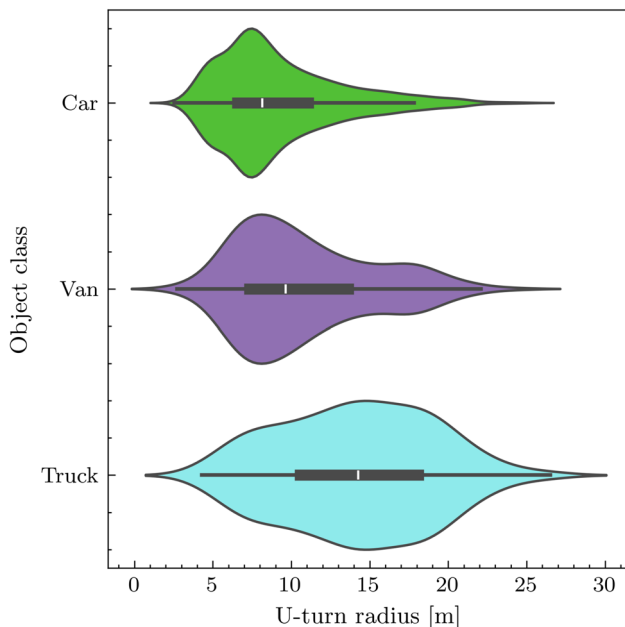
Object class	a_{min}	a_{mean}	a_{med}	a_{max}	a_{std}
Car	0.00	0.69	0.48	2.71	0.65
Van	0.00	0.58	0.41	2.42	0.55
Truck	0.00	0.48	0.36	2.28	0.45

Bold value represent the maximum values in each respective column

Table 3 Mean values of parameters at VLs (cars, N=3,663)

VL	Heading [°]	Velocity [m/s]	Acceleration [m/s ²]	Distance to the reference line [m]	Duration until next loop [s]
1st VL	10.26	3.73	0.64	1.34	10.97
2nd VL	60.09	2.90	1.14	9.19	3.26
3rd VL	186.12	5.17	1.45	5.03	1.18
4th VL	197.55	6.79	1.49	4.12	-

Bold value represent the maximum values in each respective column

**Fig. 5** Distribution of U-turn curve radius per object class

before starting the U-turn is similar. Other notable differences include the heading (cars 10°, vans 11°, trucks 57°) and the distance to the reference line (cars 1.34 m, vans 1.31 m, trucks 2.94 m) at the 1st VL. These values suggest that the U-turn maneuver of larger MRUs can be identified earlier.

As depicted in Fig. 5, a clear difference exists regarding the distance to the reference line at the 2nd loop (also referred to as curve radius).

Figure 5 presents an analysis of the U-turn radius for the three different object classes. The data is visualized using violin plots, which illustrate the distribution, density, and spread of the U-turn radius within each object class. Key characteristics of the figure are: The U-turn radius for cars is concentrated around smaller values, with a median of 8.1 m. The distribution is relatively narrow, indicating low variability. Vans show a broader U-turn radius distribution, with the median of 9.7 m. The density extends towards higher values compared to cars, reflecting greater variability in maneuvering capabilities. Trucks exhibit the largest U-turn radius, with a median of 14.3 m and a wider range of values

extending beyond 25 m. This indicates the limited maneuverability of trucks compared to the other two classes. The figure effectively highlights how the U-turn radius increases with vehicle size, emphasizing the influence of object class on maneuverability. Furthermore, the distribution of cars appears bimodal. Analysis of the video recordings suggests that the curve radius depends on the waiting position. Vehicles waiting in the second position likely have a smaller curve radius as they do not move far into the intersection while waiting for oncoming traffic.

The data also shows that the mean heading increases progressively from loop to loop, supporting the assumption that the heading serves as an indicator of the progress of the U-turn. This interpretation becomes important when analyzing parameter correlations. Out of all 400 possible pairwise correlations among the 20 parameters, based to the Pearson correlation coefficient, there are two strong, ten moderate, and 17 weak correlations.

The strongest correlation (Pearson correlation coefficient of 0.98) exists between the overall duration of the U-turn and the duration between the 1st and the 2nd VL. That indicates that the time spent for waiting for oncoming traffic is the main factor for determining the total duration of the U-turning maneuver.

At the 1st VL (when entering the intersection), the distance to the reference line shows a weak positive correlation (0.41) with the heading at the 2nd VL and a weak negative correlation (-0.31) with the heading at the 3rd VL. This suggests that a greater distance to the reference line at the 1st VL results in more of the turning maneuver is completed by the 2nd VL, and the less of the U-turn being performed between the 2nd and 3rd VLs.

The curve radius is the only parameter from the 2nd VL that exhibits at least moderate correlation with other parameters. Its positive correlation (0.78) with the heading at the 3rd VL suggests that U-turns with a smaller curve radius complete less of the turning maneuver in the second section. This is because the heading reflects the progress of the U-turn (see Fig. 6).

The positive correlation (0.57) between the curve radius and velocity at the 4th VL states that most U-turning vehicles only begin to accelerate after entering the oncoming traffic, rather than decelerating at the VRU crossing. This

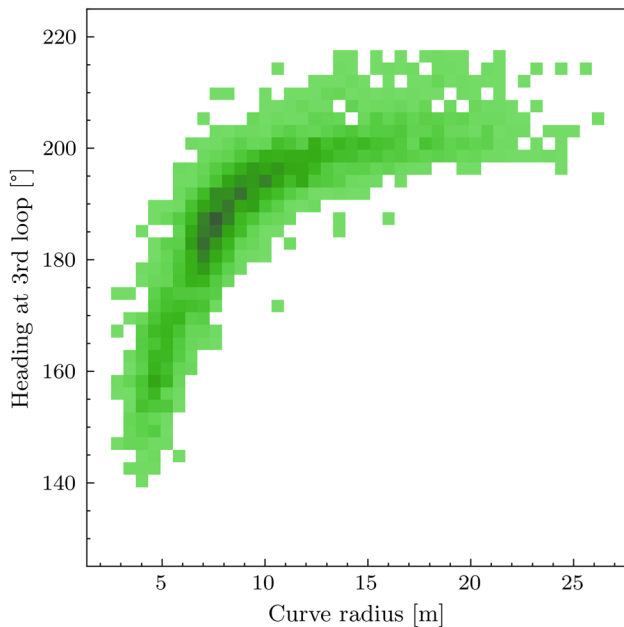


Fig. 6 Correlation between the curve radius and the heading at the 3rd VL

could indicate that vehicles tend to prioritize entering the traffic smoothly, which is relevant for a realistic simulation of real-world traffic. This behavior emphasizes the importance of calibrating the vehicle's acceleration profile to ensure safe interaction with VRUs and to avoid unexpected vehicle behavior at critical points, such as crosswalks.

At the 3rd VL, the moderate positive correlations between velocity and acceleration (0.75) as well as velocity and curve radius (0.75) suggest that vehicles with a larger curve radius have more space to accelerate before crossing the 3rd VL. This finding is important from a safety perspective, because vehicles with higher velocities might be harder to control, particularly if they need to make tight U-turns.

Beyond this, there is a strong positive correlation (0.85) between the velocities at the 3rd and 4th VL (see Fig. 7). This correlation supports the observation that, in most scenarios, there is no interaction between U-turning vehicles and VRUs between these two loops. Therefore, vehicles often accelerate between those loops and have a slightly higher velocity at the 4th than at the 3rd loop.

There is also a positive correlation (0.70) between the acceleration at the 3rd VL and the velocity at the 4th VL. That shows that vehicles accelerating at the 3rd VL are faster at the consecutive loop.

Encounters with VRUs

If we define a PET below 5 s as indicating an encounter, our data set contains 48 encounters between the U-turning MRU and crossing VRU. That means an encounter with a VRU

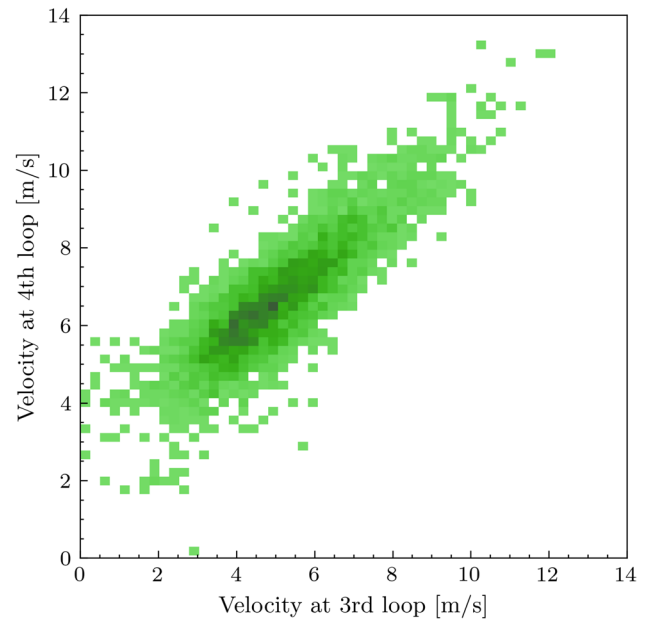


Fig. 7 Correlation between the velocities of cars at the last two VLs

occurs approximately every 84th U-turn. This low frequency of encounters underscores that interactions between the two traffic participants are relatively rare. To further investigate the likelihood of these encounters resulting in critical interactions, we will examine interactions by reducing the PET threshold in the following sections.

Moreover, encounters can be categorized based on the sign of the PET. When the PET is negative, the U-turning MRU reaches the conflict point first; conversely, when the PET is positive, the VRU arrives at the conflict point first. Figure 8 illustrates two screenshots extracted from an augmented scene video, depicting a scenario with a negative PET of -1.96 s. The camera view shows the western pedestrian crossing from south to north, where vehicle C226 performs a U-turn, crossing the pedestrian crossing after the pedestrian traffic light has turned green. The left frame captures the moment when the VRU traffic light switches to green (though not visible in the image), while the right frame, recorded 1.96 s later, shows bicyclist B595 crossing the trajectory of car C226.

Detection of Corner Cases

A threshold of an absolute PET value below 2 s is employed to identify the 15 interactions within the encounters. The relevant parameters of these interactions are presented in Table 4, sorted in ascending order by the absolute PET value. The first three columns of the table display the interaction number and the identification numbers (IDs) of the road users involved, which serve as references for the interactions. The last three numbers of the IDs are used as labels

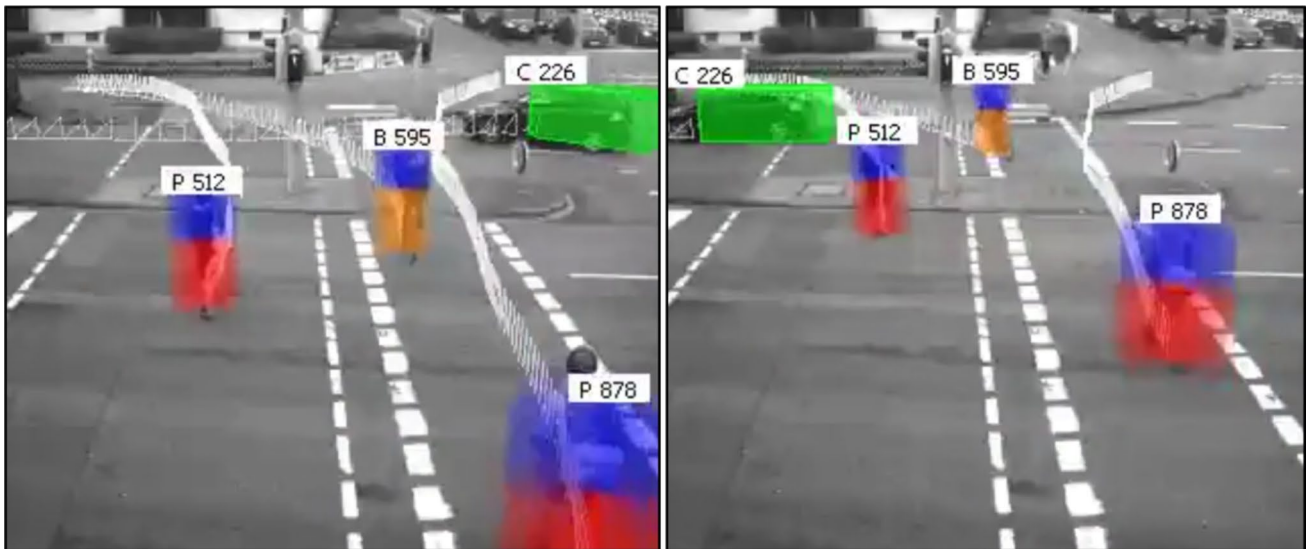


Fig. 8 Camera images of an interaction with negative PET. PET between car C226 and bicyclist B595 is -1.96 s

Table 4 Interactions with a PET between -2 s and 2 s

Index	U-turn ID	VRU ID	PET [s]	Timestamp of PET	Critical interaction
1	7,519,108	29,059,521	0.44	13.08.2019 06:44:50	Yes
2	5,354,627	20,235,408	0.68	16.07.2019 12:35:02	Yes
3	6,602,732	25,414,577	0.68	01.08.2019 17:06:15	No
4	23,140,524	110,508,213	1.20	09.05.2019 05:27:09	No
5	18,566,115	88,527,303	1.24	12.03.2019 08:20:58	No
6	635,630	2,512,288	1.24	22.05.2019 10:10:26	No
7	7,133,672	27,495,266	1.32	08.08.2019 09:01:22	Yes
8	17,612,301	83,669,586	1.48	01.03.2019 06:22:09	No
9	3,804,977	14,512,859	1.64	28.06.2019 08:03:44	No
10	1,936,893	7,541,101	1.68	06.06.2019 13:15:51	Yes
11	99,064	410,348	-1.72	03.09.2019 13:48:37	No
12	3,681,781	14,072,480	-1.76	27.06.2019 05:28:30	No
13	6,270,371	24,155,905	1.76	29.07.2019 05:59:38	No
14	19,078,226	91,132,595	-1.96	18.03.2019 07:45:47	No
15	2,279,112	8,852,732	1.96	11.06.2019 11:00:52	No

for the road users in the augmented camera images shown in Figs. 8 and 9. The fourth column lists the PET values of the interactions, while the fifth column shows the corresponding timestamp. The latter is given to illustrate the temporal distribution of situations with low PET values, emphasizing the need for several months of data recording to detect rare, critical situations. The sixth column indicates whether the interaction was classified as critical or non-critical. An interaction was classified as critical if any of the involved road users decelerated at a rate of at least 1 m/s^2 for a minimum

duration of 1 s. The results show that the four interactions classified as critical are not necessarily those with the lowest PET values. While the two interactions with the lowest absolute PET values are indeed classified as critical, the third and fourth critical interactions correspond to the seventh and tenth lowest PET values. This discrepancy highlights a limitation of the PET method, as it does not fully capture the criticality of an interaction.

In Fig. 9, the most critical situation is depicted by the camera image from the timestamp in which bicyclist B521

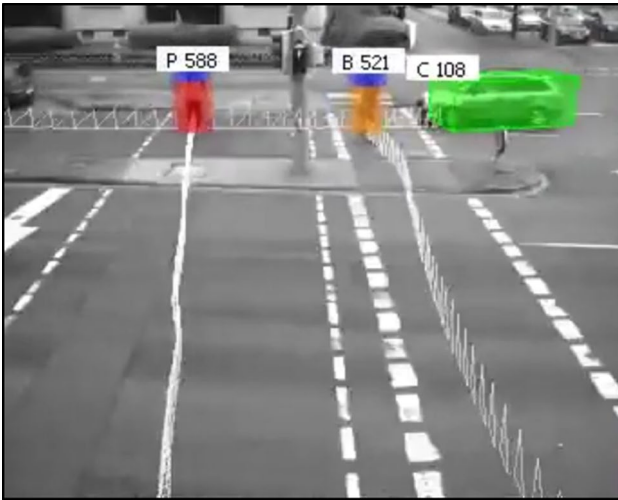


Fig. 9 Camera image of the most critical situation in the western pedestrian crossing

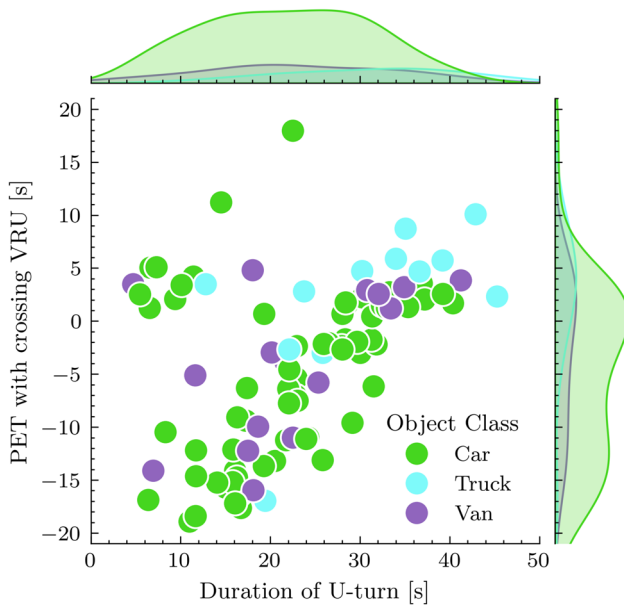


Fig. 10 Correlation between PET and duration of the U-turn

leaves the conflict area. The PET between car C108 and bicyclist B521 is 0.44 s, and the vehicle has to brake up to 3.2 m/s^2 to avoid a collision.

Camera images of the other three critical situations are depicted in Figs. 11, 12 and 13 in the Appendix. Further analysis of the video recordings of the four critical situations reveals that these incidents occur, because the U-turning MRU exit the intersection after waiting a long time for

oncoming traffic to pass. As a result, the vehicles involved in critical U-turns leave the intersection just as the traffic light for the VRUs switches from red to green. This timing issue is also indicated by the weak positive correlation (0.45) between U-turn duration and the PET, as depicted in Fig. 10.

Besides that, whereas the mean duration of all U-turns is 21 s, the mean duration of U-turns with VRU interaction is 27 s. Thus, leaving the intersection at the end of the green light phase promotes criticality. The intersection is left at the end of the green light phase when traffic volume is increased. Therefore, our results obtained from real data support the results obtained in the simulation by Olarte et al. (2011) that the number of conflicts rises with the traffic volume. What distinguishes our work most significantly is the use of large-scale real-world trajectory data to model rare critical scenarios, such as illegal U-turns, which sets our methodology apart from prior research that has typically relied on smaller data sets or theoretical models.

Furthermore, the VRUs often only consider the traffic from east to west relevant for them and do not perceive the U-turning vehicle as an object relevant to them. This aligns with the observation made by Habibovic et al. (2013) in Japan, which found that incidents involving cars and pedestrians often occur due to drivers failing to recognize pedestrians or unexpected pedestrian behavior. In addition, sometimes, the VRU does not consider any traffic, focusing solely on their traffic lights. Consequently, enhancing the awareness of MRUs regarding the traffic light status of VRUs through the utilization of hazard lights or vehicle-to-infrastructure communication has the potential to mitigate criticality in this scenario.

Finally, the data from these critical scenarios and the behavior observed during U-turns can be integrated into a scenario database for scenario-based testing. This database can serve as a valuable tool for assessing the performance of automated systems in handling such interactions. Further details on how these data will be utilized in scenario-based testing are presented in Bahn et al. (2024).

Conclusion

This work focuses on processing a large data set of naturalistic trajectories to demonstrate its application for scenario-based testing. In this context, 4,051 illegal U-turn trajectories are filtered from over 9 million trajectories of the AIM Research Intersection. The digital map of the intersection was used to extract the kinematic parameters of the traffic participants and derive parameter distributions and correlations for the descriptive modelling of the U-turn

scenario. Furthermore, the study highlights differences between U-turn maneuvers of cars, vans, and trucks, and analyzes their interactions with VRUs. By computing the PET and filtering the results, 15 interactions between motorized U-turning road users and crossing VRUs are identified. Video analysis, along with consideration of deceleration values, reveals four critical interactions all of which occur when the MRUs exit the intersection as the traffic light for VRUs changes from red to green. Proposed preventive measures such as hazard lights or vehicle-to-infrastructure communication could reduce criticality, because MRU would be informed of the VRU traffic light status.

This study addresses the research gap in understanding rare, critical scenarios such as illegal U-turns by utilizing a large real-world data set and applying scenario-based testing methods. The analysis of real-world data from these illegal scenarios lays the groundwork for future research aimed at developing strategies to enhance the resilience of automated driving systems in scenarios involving traffic rule violations by other participants. It is essential to emphasize that the instances of extracted illegal U-turns serve merely as one among numerous potential scenarios encapsulating the spectrum of illegal behaviors exhibited by road users, and thus constitute a fraction of the scenarios encompassed within a comprehensive scenario database. Nevertheless, the findings of this work demonstrate how data science can be applied in scenario-based testing to evaluate large data sets. Even rare scenarios can be identified and analyzed within a large data set. Another limitation of this study includes the specific focus on one intersection and the reliance on trajectory data that may be subject to inaccuracies. These limitations suggest that the results may not fully generalize to all urban intersections or traffic conditions.

According to the findings, waiting a long time at the intersection can create atypical situations and increase criticality. Therefore, follow-up work will look closely at other situations, where vehicles stay atypically long inside the intersection. To enhance the outcomes of this study, future work will assess whether other SSMs can better capture the level of criticality in the current scenario compared to PET. Further work will also focus on a generalization of the methodology so that parameter distributions of U-turns from other intersections can be identified based on an OpenDRIVE map.

Appendix

See Figs. 11, 12 and 13.



Fig. 11 Camera image of the second most critical situation. PET between car C627 and bicyclist B408 is 0.68 s

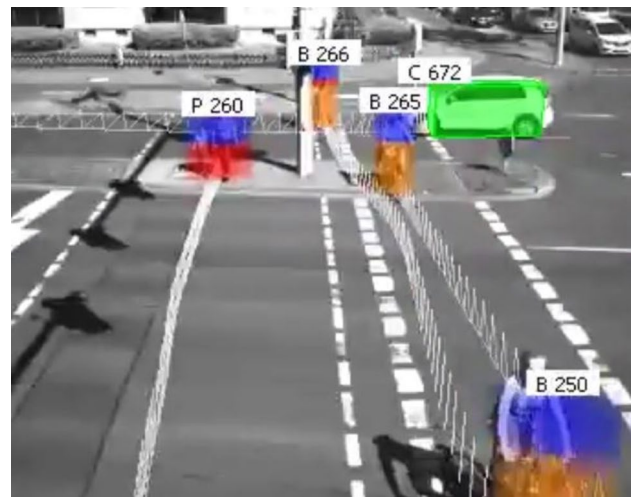


Fig. 12 Camera image of the third most critical situation. PET between car C627 and bicyclist B266 is 1.32 s

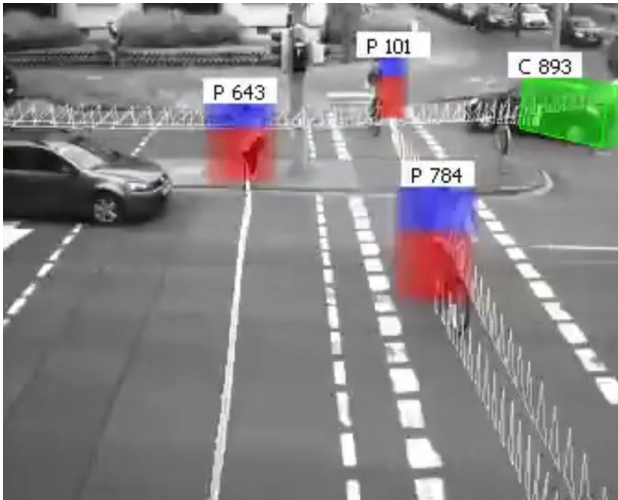


Fig. 13 Camera image of the fourth most critical situation. PET between car C893 and bicyclist P101 is 1.68 s

Acknowledgements The research leading to these results is funded by the German Federal Ministry for Economic Affairs and Climate Action within the project “Methoden und Maßnahmen zur Absicherung von KI basierten Wahrnehmungsfunktionen für das automatisierte Fahren (KI-Absicherung)”. The authors would like to thank the consortium for the successful cooperation.

Author Contributions C.S.: Methodology, software, formal analysis, writing – original draft. K.G.: Writing—reviewing and editing.

Funding Open Access funding enabled and organized by Projekt DEAL.

Data Availability No datasets were generated or analysed during the current study.

Declarations

Conflict of interest The authors have no competing interests to declare that are relevant to the content of this article.

Open Access This article is licensed under a Creative Commons Attribution 4.0 International License, which permits use, sharing, adaptation, distribution and reproduction in any medium or format, as long as you give appropriate credit to the original author(s) and the source, provide a link to the Creative Commons licence, and indicate if changes were made. The images or other third party material in this article are included in the article’s Creative Commons licence, unless indicated otherwise in a credit line to the material. If material is not included in the article’s Creative Commons licence and your intended use is not permitted by statutory regulation or exceeds the permitted use, you will need to obtain permission directly from the copyright holder. To view a copy of this licence, visit <http://creativecommons.org/licenses/by/4.0/>.

References

- Abdelhalim A, Abbas M (2022) A real-time safety-based optimal velocity model. *IEEE Open J Intell Transp Syst* 3:165–175. <https://doi.org/10.1109/ojits.2022.3147744>
- Allen BL, Shin BT, Cooper PJ (1978) Analysis of traffic conflicts and collisions. In: *Transportation Research Record*
- Al-Masaeid HR (1999) Capacity of U-turn at median openings. *Inst Transp Eng ITE J* 69(6):28
- Ansariyar A (2023) Investigating the car-pedestrian conflicts based on an innovative post encroachment time threshold (PET) classification
- Bahn B, Gimm K, Fischer M, Schicktanz C (2024). Integrierte Werkzeugkette zur Nutzung von realen verkehrlichen Szenarien für simulationsbasierte Absicherung des automatisierten Fahrens. In: *VDI Wissensforum GmbH, VDI (ed) SIMVEC - Auslegung und Absicherung von Fahrzeugsystemen*. 21. VDI-Kongress mit Fachausstellung : 19. und 20. November 2024, Baden-Baden, SIMVEC – Auslegung und Absicherung von Fahrzeugsystemen, Baden-Baden, Deutschland, 19–20 Nov 2024. Düsseldorf, VDI Verlag GmbH, pp 59–72
- Benesty J, Chen J, Huang Y, Cohen I (2009) Pearson correlation coefficient. In: *Noise reduction in speech processing*. Springer, pp 1–4
- Bogdoll D, Breitenstein J, Heidecker F, Bieshaar M, Sick B, Fingscheidt T, Zollner M (2021) Description of corner cases in automated driving: goals and challenges. In: *Proceedings of the IEEE/CVF international conference on computer vision*, pp 1023–1028
- Breitenstein J, Termohlen J-A, Lipinski D, Fingscheidt T (2020) Systematization of corner cases for visual perception in automated driving. In: *2020 IEEE Intelligent Vehicles Symposium (IV)*, Las Vegas, NV, USA, 10 Oct–13 Nov 2020. IEEE, Piscataway, NJ, pp 1257–1264
- Breitenstein J, Termöhlen J-A, Lipinski D, Fingscheidt T (2021) Corner cases for visual perception in automated driving: some guidance on detection approaches. Available online at <http://arxiv.org/pdf/2102.05897v1>.
- Breuer A, Termohlen J-A, Homoceanu S, Fingscheidt T (2020) openDD: A Large-Scale Roundabout Drone Dataset. In: *2020 IEEE 23rd International Conference on Intelligent Transportation Systems (ITSC)*, Rhodes, Greece, 20–23 Sept 2020. IEEE, pp 1–6
- Cai J, Deng W, Guang H, Wang Y, Li J, Ding J (2022) A survey on data-driven scenario generation for automated vehicle testing. *Machines* 10(11):1101. <https://doi.org/10.3390/machines1011101>
- Che Puan O, Ismail CR, Hainin MR, Minhans A, Muhamad Nor NS (2015) Midblock U-turn facilities on multilane divided highways: an assessment of driver’s merging gap and stop delays. *J Teknol*. <https://doi.org/10.11113/jt.v76.5836>
- Cres C, Zimmer W, Strand L, Fortkord M, Dai S, Lakshminarasimhan V, Knoll A (2022) A9-Dataset: multi-sensor infrastructure-based dataset for mobility research. In: *2022 IEEE Intelligent Vehicles Symposium (IV)*, Aachen, Germany, 4–9 Jun 2022. IEEE, pp 965–970
- Dixit VV, Chand S, Nair DJ (2016) Autonomous vehicles: disengagements, accidents and reaction. *PLoS ONE* 11(12):e0168054. <https://doi.org/10.1371/journal.pone.0168054>
- Elrofai H, Paardekooper J-P, de Gelder E, Kalisvaart S, den Camp OO (2018) StreetWise: scenario-based safety validation of connected automated driving
- Fagnant DJ, Kockelman K (2015) Preparing a nation for autonomous vehicles: opportunities, barriers and policy recommendations. *Transp Res Part A: Policy Pract* 77:167–181. <https://doi.org/10.1016/j.tra.2015.04.003>

- Fellendorf M (1994) VISSIM: a microscopic simulation tool to evaluate actuated signal control including bus priority. In: 64th Institute of Transportation Engineers Annual Meeting, pp 1–9
- Fraikin N, Funk K, Frey M, Gauterin F (2020) Efficient simulation based calibration of automated driving functions based on sensitivity based optimization. *IEEE Open J Intell Transp Syst* 1:63–79. <https://doi.org/10.1109/OJITS.2020.3001801>
- Guo J, Kurup U, Shah M (2020) Is it safe to drive? An overview of factors, metrics, and datasets for driveability assessment in autonomous driving. *IEEE Trans Intell Transp Syst* 21(8):3135–3151. <https://doi.org/10.1109/TITS.2019.2926042>
- Habibovic A, Tivesten E, Uchida N, Bärgrman J, Ljung Aust M (2013) Driver behavior in car-to-pedestrian incidents: an application of the driving reliability and error analysis method (DREAM). *Accid Anal Prev* 50:554–565. <https://doi.org/10.1016/j.aap.2012.05.034>
- Heidecker F, Breitenstein J, Rosch K, Lohdefink J, Bieshaar M, Stiller C, Fingscheidt T, Sick B (2021) An application-driven conceptualization of corner cases for perception in highly automated driving. In: 2021 IEEE Intelligent Vehicles Symposium (IV), Nagoya, Japan, 11–17 Jul 2021. IEEE, pp 644–651
- Kang Y, Yin H, Berger C (2019) Test your self-driving algorithm: an overview of publicly available driving datasets and virtual testing environments. *IEEE Trans Intell Veh* 4(2):171–185. <https://doi.org/10.1109/ITV.2018.2886678>
- Kassim A, Ismail K, Hassan Y (2014) Automated measuring of cyclist – motor vehicle post encroachment time at signalized intersections. *Can J Civ Eng* 41(7):605–614. <https://doi.org/10.1139/cjce-2013-0565>
- Klitzke L, Schickanz C (2024) TASI: a Python library for traffic data analysis and situation interpretation. Zenodo
- Klitzke L, Gimm K, Koch C, Koster F (2022) Extraction and analysis of highway on-ramp merging scenarios from naturalistic trajectory data. In: 2022 IEEE 25th International Conference on Intelligent Transportation Systems (ITSC), Macau, China, 8–12 Oct 2022. IEEE, pp 654–660
- Knake-Langhorst S, Gimm K (2016) AIM research intersection: instrument for traffic detection and behavior assessment for a complex urban intersection. *J Large-Scale Res Facil JLSRF*. <https://doi.org/10.17815/jlsrf-2-122>
- Kovvali VG, Alexiadis V, Zhang L (2007) Video-based vehicle trajectory data collection. In: Transportation Research Board 86th Annual Meeting
- Krajewski R, Bock J, Kloeker L, Eckstein L (2018) The highD dataset: a drone dataset of naturalistic vehicle trajectories on German highways for validation of highly automated driving systems. In: 2018 IEEE Intelligent Transportation Systems Conference. November 4–7, Maui, Hawaii, 2018 21st International Conference on Intelligent Transportation Systems (ITSC), Maui, HI, 4–7 Nov 2018. IEEE, Piscataway, NJ, pp 2118–2125
- Krajzewicz D (2010) Traffic simulation with SUMO-simulation of urban mobility. In: Fundamentals of traffic simulation. Springer, pp 269–293
- Leng J, Zhao H, Zhang Q (2009). Research on the impact of U-turn location on operation efficiency at intersection. In: Measuring Technology and Mechatronics Automation, 2009. ICMTMA '09. International Conference on, Zhangjiajie, Hunan, China, 11–12 Apr 2009. IEEE, pp 567–570
- Liu P, Wang X, Lu J, Sokolow G (2007) Headway acceptance characteristics of U-turning vehicles at unsignalized intersections. *Transp Res Rec: J Transp Res Board* 2027(1):52–57. <https://doi.org/10.3141/2027-07>
- Liu P, Qu X, Yu H, Wang W, Cao B (2012) Development of a VIS-SIM simulation model for U-turns at unsignalized intersections. *J Transp Eng* 138(11):1333–1339. [https://doi.org/10.1061/\(ASCE\)TE.1943-5436.0000438](https://doi.org/10.1061/(ASCE)TE.1943-5436.0000438)
- Maddern W, Pascoe G, Linegar C, Newman P (2017) 1 year, 1000 km: The Oxford RobotCar dataset. *Int J Robot Res* 36(1):3–15. <https://doi.org/10.1177/0278364916679498>
- Markkula G, Madigan R, Nathanael D, Portouli E, Lee YM, Dietrich A, Billington J, Schieben A, Merat N (2020) Defining interactions: a conceptual framework for understanding interactive behaviour in human and automated road traffic. *Theor Issues Ergon Sci* 21(6):728–752. <https://doi.org/10.1080/1463922X.2020.1736686>
- Martens MH, van den Beukel AP (2013) The road to automated driving: Dual mode and human factors considerations. 16th International IEEE Conference on Intelligent Transportation Systems (ITSC 2013). IEEE, The Hague, Netherlands, pp 2262–2267
- Mazaheri A, Akbarzadeh A, Rahimi AM, Akbarzadeh M (2022) Estimation of critical gap of U-turns at uncontrolled median openings considering Iran’s driver behavior. *Transp Lett* 14(1):1–13. <https://doi.org/10.1080/19427867.2020.1805680>
- Meng F, Yuan G, Lv S, Wang Z, Xia S (2019) An overview on trajectory outlier detection. *Artif Intell Rev* 52(4):2437–2456. <https://doi.org/10.1007/s10462-018-9619-1>
- Menzel T, Bagschik G, Maurer M (2018) Scenarios for development, test and validation of automated vehicles. In: 2018 IEEE Intelligent Vehicles Symposium (IV 2018). Changshu, Suzhou, China, 26–30 June 2018. IEEE, Piscataway, NJ, pp 1821–1827
- Mikhailov A, Shestеров E (2020) Estimation of traffic flow parameters of U-turns. *Transp Res Procedia* 50:458–465. <https://doi.org/10.1016/j.trpro.2020.10.054>
- Mohanty M, Dey PP (2020) Modeling the lane changing behavior of major stream traffic due to U-turns. *Transp Eng* 2:100012
- Nalic D, Mihalj T, Eichberger A, Bäumlner M, Lehmann M (2021) Scenario based testing of automated driving systems: a literature survey. In: FISITA World Congress 2021
- Olarte R, Bared JG, Sutherland LF, Asokan A (2011) Density models and safety analysis for rural unsignalised restricted crossing U-turn intersections. *Procedia Soc Behav Sci* 16:718–728. <https://doi.org/10.1016/j.sbspro.2011.04.491>
- Pearson K (1895) VII. Note on regression and inheritance in the case of two parents. *Proc R Soc Lond* 58(347–352):240–242
- Peesapati LN, Hunter MP, Rodgers MO (2013) Evaluation of post-encroachment time as surrogate for opposing left-turn crashes. *Transp Res Rec: J Transp Res Board* 2386(1):42–51. <https://doi.org/10.3141/2386-06>
- Peesapati LN, Hunter MP, Rodgers MO (2018) Can post encroachment time substitute intersection characteristics in crash prediction models? *J Saf Res* 66:205–211. <https://doi.org/10.1016/j.jsr.2018.05.002>
- Peng H, Yujing D (2020) Model of U-turn openings optimization at signalized T-intersection with single release. In: 2020 IEEE 5th International Conference on Intelligent Transportation Engineering (ICITE), Beijing, China, 11–13 Sept 2020. [S.l.], IEEE, pp 296–300
- Petrović Đ, Mijailović R, Pešić D (2020) Traffic accidents with autonomous vehicles: type of collisions, manoeuvres and errors of conventional vehicles’ drivers. *Transp Res Procedia* 45:161–168. <https://doi.org/10.1016/j.trpro.2020.03.003>
- Rathore MM, Paul A, Rho S, Khan M, Vimal S, Shah SA (2021) Smart traffic control: Identifying driving-violations using fog devices with vehicular cameras in smart cities. *Sustain Cities Soc* 71:102986
- Riedmaier S, Ponn T, Ludwig D, Schick B, Diermeyer F (2020) Survey on scenario-based safety assessment of automated vehicles. *IEEE Access* 8:87456–87477. <https://doi.org/10.1109/ACCESS.2020.2993730>
- Robicquet A, Sadeghian A, Alahi A, Savarese S (2016) Learning social etiquette: human trajectory understanding in crowded scenes. In: European conference on computer vision, pp 549–565

- Rösch K, Heidecker F, Truetsch J, Kowol K, Schick Tanz C, Bieshaare M, Sick B, Stiller C (2022) Space, time, and interaction: a taxonomy of corner cases in trajectory datasets for automated driving. In: 2022 IEEE Symposium Series on Computational Intelligence (SSCI), Singapore, Singapore, 4–7 Dec 2022. IEEE, 86–93.
- Saul H, Kozempel K, Haberjahn M (2014) A comparison of methods for detecting atypical trajectories. In: 20th international conference on urban transport and the environment, pp 393–403
- Schick Tanz C, Klitzke L, Gimm K, Mosebach HH, Liesner K (2024) DLR Urban Traffic dataset (DLR-UT). <https://doi.org/10.5281/ZENODO.11396371>.
- Schick Tanz C, Gimm K (2025) Detection and analysis of corner case scenarios at a signalized urban intersection. *Accid Anal Prev* 210:107838. <https://doi.org/10.1016/j.aap.2024.107838>
- Scholz M (2020) OpenDRIVE dataset of the inner ring road in Brunswick. <https://doi.org/10.5281/ZENODO.4043192>
- Seo T, Tago Y, Shinkai N, Nakanishi M, Tanabe J, Ushiroguchi D, Kanamori S, Abe A, Kodama T, Yoshimura S et al (2020) Evaluation of large-scale complete vehicle trajectories dataset on two kilometers highway segment for one hour duration: Zen Traffic Data. In: 2020 International Symposium on Transportation Data and Modelling
- Shahi J, Choupani A-A (2009) Modelling the operational effects of unconventional U-turns at a highway intersection. *Transportmetrica* 5(3):173–191. <https://doi.org/10.1080/18128600902795042>
- Song C-H, Lee J (2014) Detection of Illegal U-turn vehicles by optical flow analysis. *J Korean Inst Commun Inf Sci* 39C(10):948–956. <https://doi.org/10.7840/kics.2014.39C.10.948>
- Sun F, Sun L, Ma D, Wang Y, Yao R, Zeng Z (2019) Optimal location of the U-turn at a signalised intersection with double left-turn lanes. *IET Intel Transport Syst* 13(3):531–540. <https://doi.org/10.1049/iet-its.2018.5279>
- Ulbrich S, Menzel T, Reschka A, Schuldt F, Maurer M (2015) Defining and substantiating the terms scene, situation, and scenario for automated driving. *IEEE 18th International Conference on Intelligent Transportation Systems*. Gran Canaria, Spain, pp 982–988
- Wang C, Xie Y, Huang H, Liu P (2021) A review of surrogate safety measures and their applications in connected and automated vehicles safety modeling. *Accid Anal Prev* 157:106157. <https://doi.org/10.1016/j.aap.2021.106157>
- Wang W, Zhou Y, Cai Q, Zhou Y (2018) A research on detection algorithm of vehicle illegal U-turn. In: *International Conference in Communications, Signal Processing, and Systems*, pp 1089–1099
- Weber H, Bock J, Klimke J, Roesener C, Hiller J, Krajewski R, Zlocki A, Eckstein L (2019) A framework for definition of logical scenarios for safety assurance of automated driving. *Traffic Inj Prev* 20(suppl 1):S65–S70. <https://doi.org/10.1080/15389588.2019.1630827>
- Yang K, Al Haddad C, Yannis G, Antoniou C (2022) Classification and evaluation of driving behavior safety levels: a driving simulation study. *IEEE Open J Intell Transp Syst* 3:111–125. <https://doi.org/10.1109/OJITS.2022.3149474>
- Yin H, Berger C (2017). When to use what data set for your self-driving car algorithm: An overview of publicly available driving datasets. In: *IEEE ITSC 2017. 20th International Conference on Intelligent Transportation Systems: Mielparque Yokohama in Yokohama, Kanagawa, Japan, 16–19 Oct 2017*. IEEE, Piscataway, NJ, pp 1–8
- Yue B, Shi S, Wang S, Lin N (2020) Low-cost urban test scenario generation using microscopic traffic simulation. *IEEE Access* 8:123398–123407. <https://doi.org/10.1109/ACCESS.2020.3006073>
- Zernetsch S, Kress V, Bieshaar M, Reitberger G, Fuchs E, Doll K, Sick B (2022) VRU Trajectory Dataset. <https://doi.org/10.5281/ZENODO.6303669>
- Zheng C, Liu P, Lu JJ, Chen H (2009) Evaluating the effect effects of U-turns on level of service of signalized intersections using synchro and SimTraffic. In: *2009 IEEE Intelligent Vehicles Symposium, Xi'an, China, 3–5 Jun 2009*. IEEE / Institute of Electrical and Electronics Engineers Incorporated, pp 971–976
- Zhong Z, Tang Y, Zhou Y, Neves VDO, Liu Y, Ray B (2021) A survey on scenario-based testing for automated driving systems in high-fidelity simulation. Available online at <https://arxiv.org/pdf/2112.00964.pdf>
- Zhu J, Wang W, Zhao D (2018) A tempt to unify heterogeneous driving databases using traffic primitives. In: *2018 IEEE Intelligent Transportation Systems Conference, 4–7 Nov 2018 21st International Conference on Intelligent Transportation Systems (ITSC), Maui, HI*. IEEE, Piscataway, NJ, pp 2052–2057

Publisher's Note Springer Nature remains neutral with regard to jurisdictional claims in published maps and institutional affiliations.